ACS APPLIED MATERIALS & INTERFACES

Research Article

Cite This: ACS Appl. Mater. Interfaces 2019, 11, 16881−16887

www.acsami.org

Controllable Shape Changing and Tristability of Bilayer Composite

Lin Wang,[†,§,#] Dong Wang,[‡,#] Shicheng Huang,[§,#] Xing Guo,[§,∥] Guangchao Wan,[§] Jing Fan,[⊥] and Zi Chen*[,§]

[†]National Engineering Research Center for Biomaterials, Sichuan University, Chengdu 610064, China

[‡]School of Mechanical Engineering, Shanghai Jiao Tong University, Shanghai 200240, China

[§]Thayer School of Engineering, Dartmouth College, Hanover, New Hampshire 03755, United States

[∥]Key Laboratory of Advanced Technologies of Materials, Ministry of Education, School of Materials Science and Engineering, Southwest Jiaotong University, Chengdu 610031, China

[⊥]Department of Mechanical Engineering, City College of New York, New York, New York 10031, United States

Supporting Information

ABSTRACT: The programmable shape transition of a two-dimensional sheet to a three-dimensional (3D) structure in response to a variety of external stimuli has recently attracted increasing attention. Among the various shape changing materials, shape memory polymers (SMPs) can fix their temporary shape and/or their length and recover under proper thermal treatment. In this work, we create a bilayer composite by bonding one layer of elastomer with one layer of stretched SMPs, which can undergo a series of shape transitions via the storage and release of internal stresses. The programed shapes are achieved by adjusting the orientation and elongation of the SMPs. Meanwhile, the 3D structures exhibit tristability and can transit between hemihelical, left-handed helical, and right-handed helical shapes. Both theoretical analysis and finite element simulations were conducted to understand the mechanism of shape transformation and used to predict the deformed configuration by adjusting preprogramming parameters. Our work provides a new strategy and design space for fabricating smart reconfigurable structures and paves way for the design and development of bioinspired four-dimensional active matter for a broad range of applications in intelligent materials.

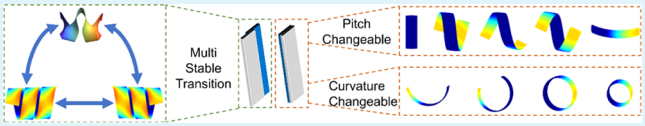

KEYWORDS: *multistable transition, shape changing, shape memory, theoretical simulation, soft robot*

INTRODUCTION

Structural transitions between multiple morphologies under external stimuli are ubiquitous in natural and engineered systems and have attracted increasing attention due to their broad applications, such as in energy harvesting, sensors, and actuators.[1−4] Examples in biology includes the fast motion of venus flytrap,[5] the folding and unfolding of pine cones,[6] and the coiling or twisting of pod seeds caused by different dehydration and orientation of cellulose fiber.[7] Their remarkable shape changing behavior has inspired scientists and engineers to develop active materials that can reconfigure in response to a variety of environmental stimuli. Stimuli-responsive polymers can change their shape upon a specific external stimulus, such as temperature, pH, light, magnetic fields, or electrical current,[1,8−10] thus becoming an outstanding candidate for smart components in sensors, actuators, or robotics with applications in aerospace and biomedical fields.[11,12] Stimuli-responsive polymers possess the unique advantages of easy processing, controllable shifting, and excellent environment sensitivity, which endow them with new strategies for fabricating multistable structures or active four-dimensional (4D) printing materials.[13,14]

Among the stimuli-responsive polymers, shape memory polymers (SMPs) and shape changing polymers (SCPs) have been most commonly studied. SMPs are able to keep a temporary shape within an appropriate temperature range and then recover the initial shape when exposed to a certain thermal stimulus.[15] SCPs can be programmed to undergo shape transition upon an appropriate stimulus, but they typically will not recover their initial shapes.[14,16,17] One example of shape changing structures is tunable helical ribbons that undergo a transition from an initially two-dimensional (2D) shape to a three-dimensional (3D) helical structure obtained by a strain engineering approach with controlled material anisotropy and geometric misorientation.[18]

By integrating active materials with geometrical design, smart structures can be developed to have preprogrammed transitions between different shapes in response to certain stimuli. Bilayer and multilayer composites containing active materials (SMPs, hydrogels) have been designed.[19] Yan et al. reported a strategy for shape changing in a continuous and reversible manner by exploiting mechanical buckling for autonomous origami assembly.[20] SMP/elastomer composites can be applied in 4D printing to fabricate self-folding, two-way shape changing structures.[21] As a new technique, ion dip-dyeing transfer printing or ink printing has been used to design

Received: December 4, 2018
Accepted: April 15, 2019
Published: April 15, 2019

DOI: 10.1021/acsami.8b21214
ACS Appl. Mater. Interfaces 2019, 11, 16881−16887

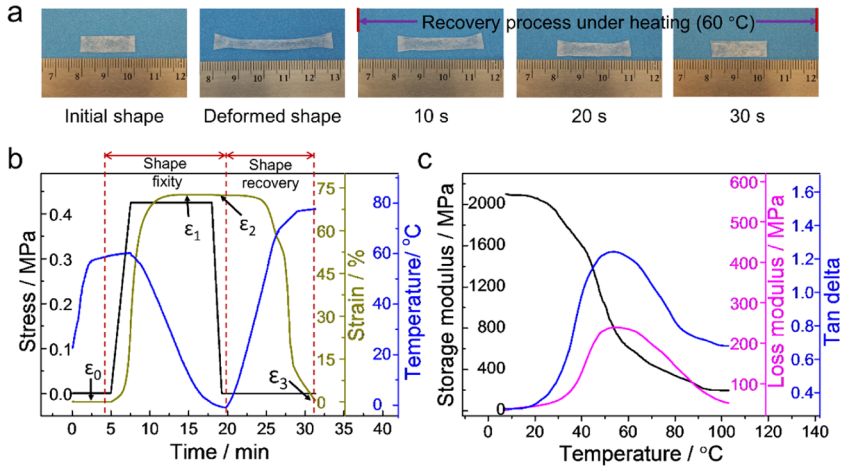

Figure 1. (a) Qualitative shape memory fixing and recover processes; (b) quantitative results of shape memory property of c-copolymer by DMA; and (c) DMA curves of c-copolymer.

complex shape transformations.[22,23] Complex 3D structures can also be created by active origami/kirigami structures.[24]

Even though several studies on the 2D−3D shape transition have been conducted, most of them only exhibit one or two stable states and there is a lack of theoretical modeling that could guide the design of the multistable structures and their shape transitions. In this work, we develop a new method to fabricate bilayer composites with stretched SMP and commercial rubber. Circle, helical, and hemihelical structures can be created by adjusting bonding areas between the rubber layer and the prestretched SMP layer. More importantly, the phenomena of multistable shape transitions between hemihelix, left-handed helix, and right-handed helix are observed for the first time to the authors' knowledge. A theoretical framework was proposed to interpret the phenomena and used to provide the design framework. Finite element simulation was also conducted to validate the transition to hemihelical shapes under thermal stimulus. Both experiments and theoretical predictions show that the bending and twisting of the helical structures can be tuned by adjusting the elongation and orientation angles of stretched shape memory cross-linked copolymer accurately. A gripper was designed based on this simple strategy, which can easily grasp and lift an object that is 30 times heavier than one actuator of the gripper under a thermal stimulus. This research paves the way for the fabrication and design of smart actuators and soft robots.

RESULTS AND DISCUSSION

Recent research mainly focuses on the shape fixity and shape recovery properties of SMPs.[15] Although traditional SMPs can change and recover their shapes in response to certain thermal treatment due to the entropy effect, it remains challenging to keep the deformed 3D structure fixed at a desirable temperature.[25] What will happen during their recovery process if the stretched shape memory polymer is bonded with general rubber or other elastomers? New structures may be generated due to the constraint during the recovery process. Here, we studied the shape transformation of bilayer composite, which consisted of stretched shape memory c-copolymer and a commercial elastomer with different bonding manners, elongations, and orientations.

A series of copolymers were synthesized by radical polymerization with butyl acrylate (BA), 2-hydroxyethyl acrylate (HEA), and cinnamoyloxyethyl acrylate (CEA) as reaction monomer and 2,2-azoisobutyronitrile (AIBN) as initiator (Schemes S1 and S2). The chemical structures of CEA and copolymer were measured by ^{1}H NMR. The results of integrated area and the characteristic chemical shifts in ^{1}H NMR spectra (Figures S1 and S2) confirmed that CEA and copolymer were successfully synthesized. Photo-cross-linked copolymer (c-copolymer) can be formed upon UV irradiation with the wavelength of λ = 365 nm for 100 min. The results of UV−vis absorption spectra (Figure S3) of copolymer with different irradiation times further indicate the formation of cross-linking structure. By comparing the absorbance at 274 nm with different irradiation time intervals, the degree of photo-cross-linking is 65% after 100 min irradiation. The c-copolymer possesses a wide transition temperature range, which, from the results of differential scanning calorimetry (DSC) (Figure S4) and dynamic mechanical analysis (DMA), endow the c-copolymer with a good shape memory property.[26] Both the results of qualitative experimental shape memory process (Figure 1a) and quantitative DMA shape memory programming (Figure 1b) indicate the c-copolymer with excellent shape memory property. The shape fixity ratio (R_f) and shape recovery ratio (R_r) of the shape memory cycles are calculated by eqs 1 and 2

$$R_f = \frac{l_2}{l_1} \times 100\% \quad (1)$$

$$R_r = \left(1 - \frac{l_3}{l_2}\right) \times 100\% \quad (2)$$

where l_0, l_1, l_2, and l_3 represent the initial length, stretched length, fixed length, and recovered length, respectively. The R_f and R_r of c-copolymer with 10% CEA content and 100 min irradiation time can reach up to 95%. We also studied the recovery stress by DMA with an isostrain mode. Figure S5 shows that the recovery stress first increased with increasing applied temperature, and then decreased because of the stress relaxation. The maximum recovery stress in the recovery process can reach up to 1.15 MPa.

Next, two methods were proposed to fabricate the bilayer composite (Figure S6). One is fully bonding rubber strip and stretched shape memory c-copolymer with different misorientation angles and different elongations. The other is by

DOI: 10.1021/acsami.8b21214
ACS Appl. Mater. Interfaces 2019, 11, 16881−16887

partial bonding between rubber and stretched shape memory c-copolymer with a tensile strain of 125%. The c-copolymer/rubber bilayer strips can be used as an efficient tool to realize three-dimensional transformation by generating internal stress due to material and geometrical heterogeneity. As shown in Figure 2, all of the bilayer composites could maintain their bonded shapes at a low temperature (20 °C). Upon heating, the bilayer composite would deform into different structures depending on the initial setup. The bilayer strip with a full bonding between an stretched c-copolymer with an tensile strain of 125% and rubber will form a circle when the misorientation angle between the two layers is 0° (Figure 2a). A helical shape can form by a fully bonded bilayer strip with a misorientation angle of 45° (Figure 2b). Besides, partially bonded bilayer strip deformed into a hemihelical shape with one perversion upon heating (Figure 2c).

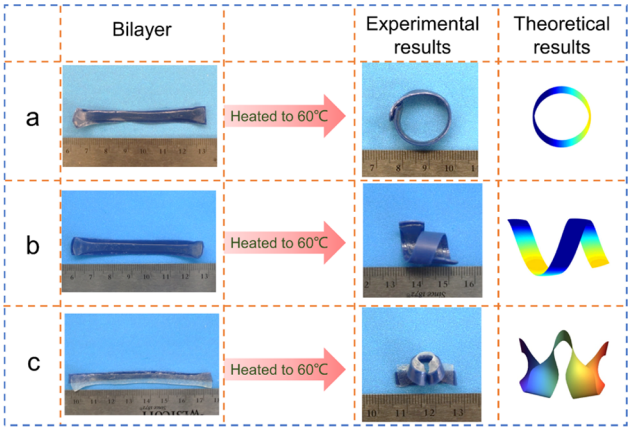

Figure 2. Shape transitions and theoretical results of (a) fully bonded with orientation angle at 0°, (b) fully bonded with orientation angle at 45°, and (c) partially bonded bilayer strips under thermal stimulation.

We further examined the effect of the tensile strain of c-copolymer and misorientation angle on shape changing of bilayer composite. Helical shapes with different radius and pitch can be formed by full-bonded bilayer strips with different tensile strain of c-copolymer and cutting angle. The experimental changed and theoretically predicted shapes of the full-bonded bilayer strips with different orientation angles θ = 0, 15, 30, 45, 60, 75, and 90° are shown in Figures 3a and S7. The pitch of the helical shape increased from 0 to 15 mm with an increase of orientation angle from 0 to 60°, then back to 0 mm when further increasing orientation angle from 60 to 90°. The helix angle of helical shape increased from 0 to 90° with an increase of orientation angle from 0 to 90°. The lateral bending is not obvious compared to the bending in longitudinal direction, due to the fact that the curvature in transverse direction is generally much smaller than that in the longitudinal direction as the bilayer deformed and the width is much less than the length. For the case of 90, the width is relatively larger and it can be seen clearly from both experimental and theoretical results that the lateral bending exists. Moreover, the curvatures of changed shape increase from 86.96 to 235.29 m^{-1} with prestretched tensile strain in the range of 50−200% (Figure 3b). The theoretical result was highly consistent with the experimental result in pitches, helix angles, and curvatures of the formed helical structures (Figure 4). It should be noted that the orientation angle in the theoretical results in Figure 4c is set as 0° and compared with the experimental results of the fully bonded bilayer with orientation angle as 0°. We also found that the experimentally measured curvatures are smaller than the theoretical results when the prestretched tensile strain is 75, 100, or 200%. The discrepancy in curvature is due to larger stress relaxation and increasing energy loss under larger tensile strain.[27]

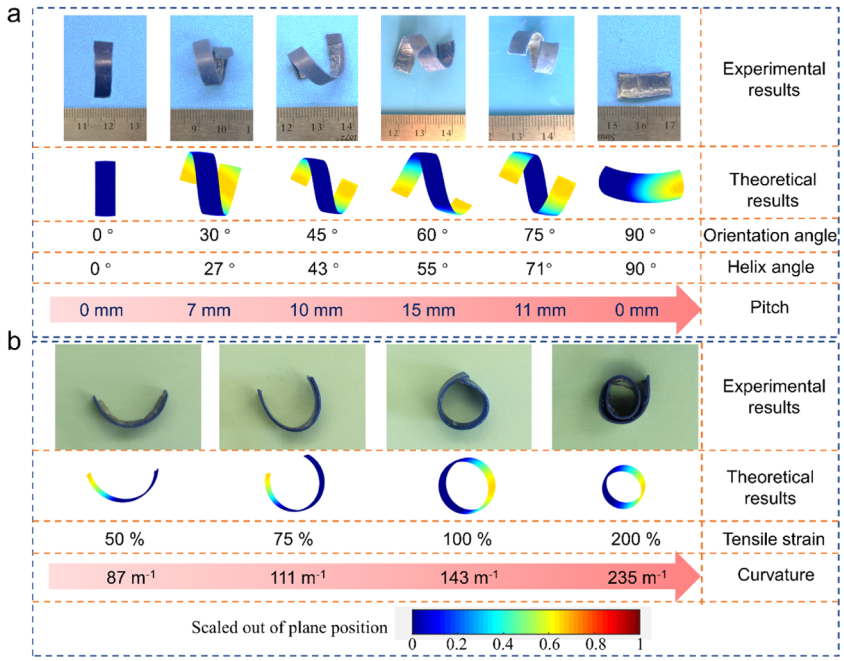

Figure 3. Experimental and theoretical results of full-bonded bilayer strips with (a) different orientation angles θ = 0, 30, 45, 60, 75, and 90° and (b) different tensile strains of c-copolymer.

DOI: 10.1021/acsami.8b21214
ACS Appl. Mater. Interfaces 2019, 11, 16881−16887

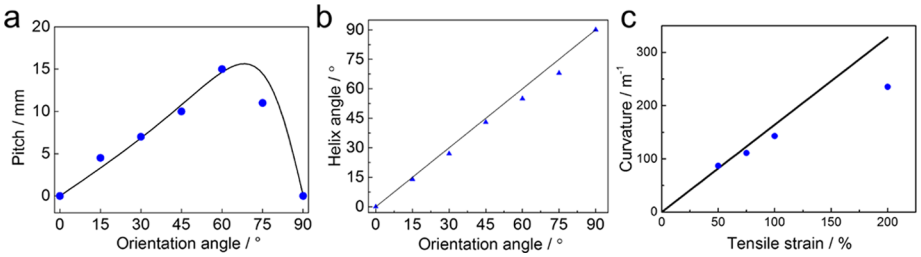

Figure 4. Theoretical and experimental results: (a) pitch−angle curve, (b) helix angle−orientation angle, and (c) curvature−tensile strain curve of bilayer composite.

To understand the helical structures formed by the fully bonded bilayer strips with different layer orientations upon heating, a theoretical model based on minimum potential energy was used. Upon heating, the shape memory c-copolymer tended to contract and thus generated an internal stress **f** on the interface between the rubber and c-copolymer with its magnitude f as

$$f = -E_p(\varepsilon_2 - \varepsilon_3) \tag{3}$$

where E_p is Young's modulus of the SMP, ε_2 is the strain before heating, and ε_3 is the recovered strain of a single strip of SMP. Here, we assume the polymers are linear elastic and neglect their viscous and nonlinear part. The potential energy of the strip is then given as

$$\prod = -\mathbf{WHLf}: \gamma|_{z=-H/2} + WL\int_{-H/2}^{H/2} \frac{1}{2}\gamma: \mathbf{C}: \gamma \, dz \tag{4}$$

where W, H, and L are the width, height, and length of the bilayer, respectively, and **C** is the effective fourth-order elastic stiffness tensor of the bilayer composite. Here, z denotes the thickness direction. The strain γ can be represented in the principal coordinates ($\mathbf{r}_1$, $\mathbf{r}_2$, $\mathbf{r}_3$) as

$$\gamma = \begin{pmatrix} \varepsilon_{11} + z\kappa_1 & 0 & 0 \\ 0 & \varepsilon_{22} + z\kappa_2 & 0 \\ 0 & 0 & \varepsilon_{33} + qz \end{pmatrix} \tag{5}$$

where ε_{11}, ε_{22}, and ε_{33} represent the strain in $\mathbf{r}_1$, $\mathbf{r}_2$, and $\mathbf{r}_3$ directions, respectively, at $z = 0$ plane; κ_1, κ_2 represent the bending curvature; and q is required for plane stress compatibility. Here, we assume plane stress and the transverse shear on the surface of the bilayer vanishes because the thickness of the bilayer is thin comparing to the length and width dimensions. However, the transverse shear may be important and the effect of the transverse shear can be further studied in the future work.

By minimizing the total potential energy density with respect to the seven unknowns ε_{11}, ε_{22}, ε_{33}, κ_1, κ_2, q, and $\varnothing$, a solution with a helical deformed structure can be found as

$$\phi = \theta,\ \kappa_1 = \frac{6f}{E_{\text{eff}}H},\ \kappa_2 = \frac{-6\nu f}{E_{\text{eff}}H},\ q = -\frac{6\nu f}{E_{\text{eff}}H},$$
$$\varepsilon_{11} = -\frac{f}{E_{\text{eff}}}, \varepsilon_{22} = \frac{\nu f}{E_{\text{eff}}},\ \varepsilon_{33} = \frac{\nu f}{E_{\text{eff}}} \tag{6}$$

where E_{eff} and ν_{eff} are the effective Young's modulus and Poisson ratio, respectively. The pitch and curvature for the helical shape can then be derived as[28]

$$P = 2\pi\sqrt{\frac{(\kappa_1 - \kappa_2)^2 \sin(2\phi)^2}{(\kappa_1^2 + \kappa_2^2 + (\kappa_1 - \kappa_2)(\kappa_1 + \kappa_2)\cos(2\phi))^2}} \text{ and}$$
$$R = \sqrt{\frac{(\kappa_1 + \kappa_2 + (\kappa_1 - \kappa_2)\cos(2\phi))^2}{(\kappa_1^2 + \kappa_2^2 + (\kappa_1 - \kappa_2)(\kappa_1 + \kappa_2)\cos(2\phi))^2}} \tag{7}$$

The theoretical predictions deformation of (a) fully bonded with orientation angle at 0°, (b) fully bonded with orientation angle at 45°, and (c) partially bonded bilayer under thermal simulation are plotted in the last column in Figure 2 and compared to the experimental results. Theoretical predicted shapes exhibit similar helical behaviors to those in experiments. Next, we quantitatively compared the experimental and theoretical results. The dependence of the theoretically predicted pitch/curvature is shown in Figure 4 and compared to the experimentally measured pitch/curvature. Theoretical prediction agrees well with the experiments. Theoretical prediction shows that the pitch increases from 0 at $\theta = 0°$ until it reaches its maximum at $\theta = \sim 68°$ when the orientation angle increases. Then, the pitch decreases from its maximum to 0 at $\theta = 90°$. The theoretical results thus could provide design guidelines. If a maximum pitch is required for this type of soft actuators, an orientation angle of ~68° could be used. The theoretically predicted curvature is linearly proportional to the elongation with orientation angle $\theta = 0°$, which agrees with the experiments.

Experiments also indicate that under a small perturbation, the hemihelical shape could transform to left-handed or right-handed helical structures at 65 °C, as shown in Figure 5a. This phenomenon shows that the deformed hemihelical shape exhibits multistability and all of the hemihelical, left-handed, and right-handed helical structures are stable states. To understand the formation of the hemihelical structure and the multistable transitions, the kinematics of the bilayer strip should be considered. Here, a different model based on Kirchhoff's theory of rods is used.[29] Because the overlap in the partial bond is small, we assume that the two strips are aligned side by side for simplification. Under the effect of heat, the strips will initially be curved with a natural curvature $K = \frac{12(\varepsilon_2 - \varepsilon_3)}{8w(\varepsilon_2 - \varepsilon_3 + 2)}$ and a length of $L = \frac{8(\varepsilon_2 - \varepsilon_3 + 2)}{(\varepsilon_2 - \varepsilon_3)^2 + 16(\varepsilon_2 - \varepsilon_3) + 16}l$, by assuming that the stiffnesses of the two layers are comparable.[29] However, this curved structure is not stable under a small perturbation and it will transition to a stable hemihelical structure. As the strip is in static equilibrium, the force and moment balance require

$$\mathbf{F}' = 0 \tag{8}$$

$$\mathbf{M}' + \mathbf{d}_3 \times \mathbf{F} = 0 \tag{9}$$

DOI: 10.1021/acsami.8b21214
ACS Appl. Mater. Interfaces 2019, 11, 16881−16887

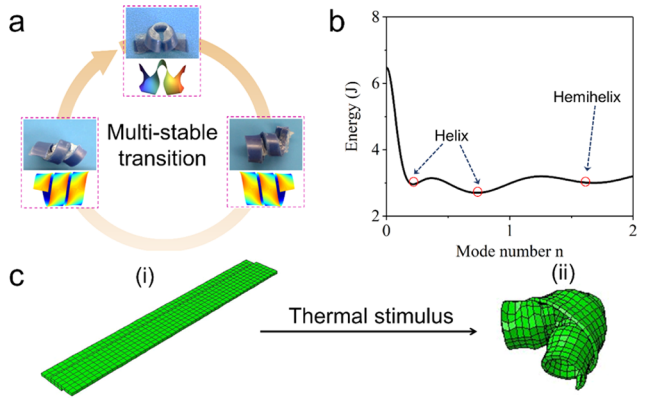

Figure 5. (a) Hemihelix structure formed by partially bonded strips exhibit multistability by changing to left-handed and right-handed helical structures; (b) schematics of the change of energies with mode number *n*. The energies for different stable states: helix and hemihelix are local minimums; (c) finite element simulations to validate the transition from bilayer strip (i) to hemihelical shape (ii) under heating.

where $\mathbf{F} = F_1\mathbf{d}_1 + F_2\mathbf{d}_2 + F_3\mathbf{d}_3$ is the resultant force, $\mathbf{M}$ is the resultant moment acting on the cross section, and ($\mathbf{d}_1$, $\mathbf{d}_2$, $\mathbf{d}_3$) are orthonormal coordinates located on the bilayer strips, where $\mathbf{d}_1$ is along the length direction, $\mathbf{d}_2$ is along the width direction, and $\mathbf{d}_3$ is along the thickness direction. The composite strip is linear elastic, thus

$$\mathbf{M} = E_{\text{eff}} I_1(\kappa_1 - K)\mathbf{d}_1 + E_{\text{eff}} I_2 \kappa_2 \mathbf{d}_2 + G_{\text{eff}} J \kappa_3 \mathbf{d}_3 \tag{10}$$

where I_1 and I_2 are the principal moments of inertia of the cross section of the bistrip, E_{eff} and G_{eff} are the effective Young's modulus and shear modulus, respectively, and J is the torsion constant. The equilibrium shape of the bistrip is investigated by perturbation theory up to second order. The deformed shape can be represented as (Theory part, Supporting Information)

$$x = \begin{pmatrix} -\dfrac{GJ \sin(w_n s)}{w_n(EI_1^2K^2 - EI_2GJw_n^2)} \\ \dfrac{EI_1GJK(-3EI_1^2K^2 + EIGJw_n^2 + 5EI_2GJw_n^2 - 2GJ^2w_n^2)\cos(2w_n s)}{4w_n(EI_1^2K^2 - EI_2GJw_n^2)^2(EI_1^2K^2w_n + EI_1GJw_n^3 - EI_2GJw_n^3)} \\ s - \dfrac{GJ^2 \sin(2w_n s)}{4w_n(EI_1^2K^2 - EI_2GJw_n^2)^2} \end{pmatrix} \tag{11}$$

where $w_n = n\pi/L$ is the angular frequency of the corresponding mode. The predicted hemihelix shape is plotted using the above equations in Figure 2 with normalized parameters.

It was found that the hemihelical shape could transform to a left-handed or right-handed structure at 65 °C in experiments. To understand this behavior, the energy of the system is plotted against the mode *n* from 0 to 2 (Figure 5b). Several stable states with local minimum energy exist at n = ~0.2, 0.7, and 1.6. It has been indicated in ref 29 that the mode number *n* represents the number of perversions in the final shape and noninteger values of *n* means that the number of perversion of the strip equals the integer part of *n* and there is a perversion lying outside of the strip, which accounts for the noninteger part. At n = ~1.6, the stable state is a hemihelix structure with one perversion (Figure 5a). At n = ~0.2 and ~0.7, the perversion in hemihelix structure lies outside of either the left or right side of the bistrip. Thus, a right-handed or left-handed helix segment forms.[29] By a small perturbation, the energy gap can be overcome and the three stable states, hemihelix, right-handed, and left-handed helix, can be transformed. Different fabrication methods could also affect the stability of the bistrips. For small overlap in partial bonding, the hemihelical structure has less energy than left-handed/right-handed structures and will be the most stable state, while left-handed/right-handed structures will be more stable with larger overlap in partial bonding. It should be noted that the number of turns in the helical shape is also affected by self-contact of the structure, which is not incorporated in our theoretical model.

However, it can be seen from Figure 5b that the stable shapes have similar energy level and the energy barriers between different stable shapes are relatively low. This is because the self-contact between the surface of the bilayer is not taken into account, which may increase the energy barriers. To further investigate the effect of self-contact on the multistability of the bilayer, finite element simulations were performed to validate the transition to hemihelical shape by using the commercial software ABAQUS, as shown in Figure 5c and Video 1. The details of the finite element simulation are shown in the Supporting Information. The initial state is a partially bonded bilayer strip. Both materials in both layers are assumed to be linear elastic. The shape memory polymer layer is set to be temperature-sensitive. A small perturbation is applied in the simulation to trigger different stable states. As temperature decreases gradually, a hemihelical shape is formed. It can be observed that there is a chirality transformation in the strip, which starts from one handiness and ends with another handiness and involves complex self-contact.

We assembled a soft gripper, which consisted of two fully bonded stretched shape memory c-copolymers and rubber strips as shown in Figure 6. Under thermal stimulation, the soft gripper will bend and form a circular arc. Therefore, it can easily catch and lift a cylinder that is 30 times heavier than its weight.

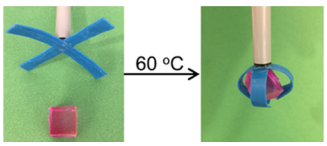

Figure 6. Soft gripper assembled by two bilayer can catch and lift an object under thermal stimulus.

EXPERIMENTAL SECTION

Materials. 2-Hydroxyethyl acrylate (HEA) (97%), cinamoyl chloride, 2,2-azoisobutyronitrile (AIBN), anhydrous tetrahydrofuran (THF), triethylamine (TEA), anhydrous sodium sulfate (Na_2SO_4), and diethyl ether were purchased from Sigma. Butyl acrylate was purchased from Alfa, and AIBN was purified by recrystallization from ethanol before use. Devcon 5-Minute Epoxy was purchased from Devcon Corp. Commercial rubber with Young's modulus of 1.34 MPa was used.

Characterization Methods. ^{1}H NMR spectra were recorded on a Bruker AM-500 MHz spectrometer. Chemical shifts are expressed in ppm (δ), and $CDCl_3$ was used as the testing solvent. The ultraviolet−visible (UV−vis) spectra of the copolymer were recorded on a Shimadzu UV-2550 spectrophotometer. The photo-cross-linking degree can be calculated by comparing the absorption intensity at 274 nm in different irradiation intervals. We use a TA DSC-Q200 to measure the thermal properties of the copolymers from 10 to 150 °C,

DOI: 10.1021/acsami.8b21214
ACS Appl. Mater. Interfaces 2019, 11, 16881−16887

and we use a second round of heating and cooling processes to eliminate the thermal history. Dynamic mechanical properties were measured by using a standard testing specimen with size of 20 mm × 5 mm × 0.5 mm on a TA DMA-Q800, with a heating rate of 3 °C·min^{-1} and a heating range of −5−105 °C (1 Hz). The tan δ, storage modulus, and loss modulus were recorded. The static tensile tests of c-copolymer were measured on a universal testing machine Instron 4464 with a speed of 10 mm·min^{-1}. The shape fixity and recovery strains were tested on a TA DMA-Q800 with the controlled force mode by using designed program as follows.[22] First, the sample (ε_0) was equilibrated at 60 °C for 3 min and stretched from 0 to 0.42 MPa with a stretch rate of 0.2 MPa·min^{-1} to obtain a temporary stretched sample, marked as ε_1; second, the final fixed shape was obtained by cooling the stretched sample and releasing the applied stress, marked as ε_2. Finally, the recovery strain was obtained by reheating the fixed strain at 75 °C, marked as ε_3. The R_f and R_r can be calculated according to eqs 1 and 2.

Preparation and Characterization of Cross-Linked Copolymer (c-Copolymer). *Synthesis of Cinnamoyloxyethyl Acrylate (CEA).* CEA was synthesized by an esterification of HEA and cinnamoyl chloride in anhydrous THF, where TEA was used as base (Scheme S1). Briefly, HEA (5 mL), TEA (4.5 mL), and THF (40 mL) were added into a 250 mL three-neck flask, cinnamoyl chloride (7 g) was taken in a 100 mL addition column with 20 mL of THF added dropwise to the flask for 10 min. The reaction was kept in an ice bath for 3 h, then for 4 h at room temperature. The filtrate was obtained by filtering off the TEA−HCl salt and extracted with diethyl ether; then, the diethyl ether layer was dried with anhydrous Na_2SO_4 overnight, and the final oily monomer was obtained by evaporating the diethyl ether filtrate, in a yield of 50%.

Synthesis of Poly((butyl acrylate)-(cinnamoyloxyethyl acrylate)) (Poly(BA-HEA-CEA)). Synthesis of poly(BA-HEA-CEA) was carried out in ethanol with AIBN as an initiator by free-radical copolymerization (Scheme S2A). Briefly, certain amounts of CEA, HEA, BA, and AIBN were added to a three-neck flask, nitrogen was flown through the solution for 10 min before polymerization, and the reaction was conducted under 60 °C for 2 h. The copolymer was obtained by reprecipitation, washed with distilled water, and dried under vacuum.

Photo-Cross-Linking of Poly(BA-HEA-CEA) (c-Copolymer). The poly(BA-HEA-CEA) is a kind of photosensitive polymer; since the cinnamon group is a photoreversible group, two groups can form a cross-linking structure upon irradiation of 365 nm UV light (Scheme S2B). c-Copolymer was prepared by irradiating the poly(BA-HEA-CEA)/DMF solution by using a 365 nm UV light for 100 min; then, the cross-linked polymer was dried in vacuum for 1 day to obtain a film. To indicate the formation of the cross-linking structure, poly(BA-HEA-CEA) in DMF solution was measured by UV−vis absorption spectrum (Figure S3, Supporting Information); the cinnamon group in the copolymer has a maximum absorption at 274 nm. Besides, the results further demonstrated the successful preparation of the c-copolymer and the cross-linking structure endow the c-copolymer with good thermally induced shape memory effect.

Effect of Cinnamon Content and Irradiation Time on Shape Memory Effect. We studied the effect of different cinnamon content and irradiation time on R_f and R_r of c-copolymer. The samples with different cinnamon contents and irradiation times were denoted as *P-x-y*, where *x* is the molar percentage of cinnamon group in all acrylate groups (the molar percentage of CEA in BA, HEA and CEA) (%) and *y* is the irradiation time (min). As shown in Table S1, both R_f and R_r increased with increasing cinnamon content and irradiation time due to the occurrence of more [2 + 2] cycloaddition reaction under increasing irradiation time and induced the c-copolymer with an increased cross-linked structure. Here, we chose c-copolymer with 10% CEA content and 100 min as irradiation time for further study since both the R_f and R_r of P-10-100 can reach up to 95%. In this part, the shape memory effect was measured as follows. First, the rectangular strip samples with dimensions of 40 mm × 5 mm × 0.5 mm (ε_0) were stretched to 60% (ε_1) at 65 °C and fixed by cooling to 0 °C (ε_2); then, the stretched specimens were placed in an oven at 65 °C and the length of the recovery specimen (ε_3) was measured. The experiment was repeated at least three times and the R_f and R_r values were calculated by using eqs 1 and 2.

To determine the shape changing temperature (shape memory transition temperature) of c-copolymer, DSC and DMA were tested. From the DSC result of c-copolymer (Figure S4, Supporting Information), there is a wide glass-transition temperature area from 30 to 115 °C, indicating that the c-copolymer has a good shape memory property. The result of DMA (Figure 1c) showed that the storage modulus decreased from 2100 to 220 MPa with increasing temperature from 25 to 100 °C, further confirming the wide temperature range of transition temperature. Moreover, the significant difference in storage modulus at different temperatures also endowed the polymer a good shape memory property. Next, we studied the thermal-induced shape memory process of c-copolymer. Figure 1a shows that the c-copolymer sample with a length of 2 cm was stretched to 4.7 cm at 60 °C, then the deformed shape can be obtained by cooling the stretched polymer at 0 °C for 10 s; the deformed shape would recover its initial length when the deformed specimen was stimulated by heating (60 °C) in 30 s. Quantitative results of shape memory property of c-copolymer were measured by DMA (Figure 1b), and the sample (ε_0) was stretched to ε_1 at 60 °C, then cooled down to 0 °C, releasing the applied load, a fixed shape (ε_2) was obtained, and the recovered shape was obtained (ε_3) when the fixed shape was reheated. From eqs 1 and 2, R_f and R_r are 98.8 and 98.3%, respectively, indicating the excellent shape memory property of c-copolymer.

Fabrication of c-Copolymer/Rubber Bilayer Composite. Two fabrication methods are presented to fabricate the bilayer composite, as shown in Figure S6. Rubber and stretched c-copolymer are bonded by using Devcon 5-Minute Epoxy and held for 1 h at room temperature. The first method is fully bonded of rubber strip and stretched shape memory c-copolymer with different orientation angles and different elongations. The second method is by partially bonded between rubber and stretched shape memory c-copolymer with a tensile strain of 125%.

CONCLUSIONS

In summary, we synthesized a shape memory copolymer and used its shape memory effect to fabricate an SMP/rubber bilayer composite that exhibits 2D to 3D structure transition and multistability. Two fabrication methods are proposed as fully bonded and partially bonded. The full bonding method can be used to create helical structures with different twists, pitches, and/or curvatures accurately by adjusting the orientation angle and/or elongation of c-copolymer. The partial bonding method is used to construct hemihelical and multistable structures. Theoretical models are proposed to study all of the helical and hemihelical structures as well as the multistability of the partially bonded bilayer strips. The novelty of the theoretical modeling is that: (1) the theoretical results in model for a fully bonded strip illustrate how the orientation angles affect the pitch and radius of the deformed shape; (2) based on the model for a partially bonded bilayer, we use the theoretical energy to show the possibility of multistability. Finite element simulations are further conducted to explore the transition of a partially bonded bilayer strip to hemihelical configuration, taking into account self-contact. This simple method provides a new strategy to fabricate complex geometric structures and can be extended to the fields of self-folding origami, 4D printing, soft actuators and robots, and biomedical engineering.

DOI: 10.1021/acsami.8b21214
ACS Appl. Mater. Interfaces 2019, 11, 16881−16887

■ ASSOCIATED CONTENT

Supporting Information

The Supporting Information is available free of charge on the ACS Publications website at DOI: 10.1021/acsami.8b21214.

Finite element simulations to validate the transition from bilayer strip to hemihelical shape under heating (AVI)

Theoretical analysis; effect of width and thickness aspect ratio on hemihelical/helical bifurcation; energy conversion efficiency; finite element simulations (PDF)

■ AUTHOR INFORMATION

Corresponding Author

*E-mail: Zi.Chen@dartmouth.edu.

ORCID

Zi Chen: 0000-0001-5927-0249

Author Contributions

#L.W., D.W., S.H. contributed equally.

Funding

Startup fund from the Thayer School of Engineering at Dartmouth and the support from the Branco Weiss−Society in Science Fellowship, administered by ETH Zürich. ACS Petroleum Research Fund and CUNY Advanced Science Research Center.

Notes

The authors declare no competing financial interest.

■ ACKNOWLEDGMENTS

Z.C. acknowledges the startup fund from the Thayer School of Engineering at Dartmouth and the support from the Branco Weiss−Society in Science Fellowship, administered by ETH Zürich. J.F. acknowledges the support from ACS Petroleum Research Fund and CUNY Advanced Science Research Center.

■ REFERENCES

(1) Lu, W.; Le, X.; Zhang, J.; Huang, Y.; Chen, T. Supramolecular Shape Memory Hydrogels: a New Bridge between Stimuli-responsive Polymers and Supramolecular Chemistry. *Chem. Soc. Rev.* **2017**, *46*, 1284−1294.

(2) Guo, Q.; Bishop, C. J.; Meyer, R. A.; Wilson, D. R.; Olasov, L.; Schlesinger, D. E.; Mather, P. T.; Spicer, J. B.; Elisseeff, J. H.; Green, J. J. Entanglement-Based Thermoplastic Shape Memory Polymeric Particles with Photothermal Actuation for Biomedical Applications. *ACS Appl. Mater. Interfaces* **2018**, *10*, 13333−13341.

(3) Zhang, W. M.; Yan, H.; Peng, Z. K.; Meng, G. Electrostatic Pull-in Instability in MEMS/NEMS: a Review. *Sens. Actuators, A* **2014**, *214*, 187−218.

(4) Jeon, S.-J.; Hauser, A. W.; Hayward, R. C. Shape-morphing Materials from Stimuli-responsive Hydrogel Hybrids. *Acc. Chem. Res.* **2017**, *50*, 161−169.

(5) Forterre, Y.; Skotheim, J. M.; Dumais, J.; Mahadevan, L. How the Venus Flytrap Snaps. *Nature* **2005**, *433*, 421−425.

(6) Harrington, M. J.; Razghandi, K.; Ditsch, F.; Guiducci, L.; Rueggeberg, M.; Dunlop, J. W.; Fratzl, P.; Neinhuis, C.; Burgert, I. Origami-like Unfolding of Hydro-actuated Ice Plant Seed Capsules. *Nat. Commun.* **2011**, *2*, No. 337.

(7) Armon, S.; Efrati, E.; Kupferman, R.; Sharon, E. Geometry and Mechanics in the Opening of Chiral Seed Pods. *Science* **2011**, *333*, 1726−1730.

(8) Chen, Q.; Yu, X.; Pei, Z.; Yang, Y.; Wei, Y.; Ji, Y. Multi-stimuli Responsive and Multi-functional Oligoaniline-modified Vitrimers. *Chem. Sci.* **2017**, *8*, 724−733.

(9) Kaiser, S.; Radl, S.; Manhart, J.; Ayalur-Karunakaran, S.; Griesser, T.; Moser, A.; Ganser, C.; Teichert, C.; Kern, W.; Schlögl, S. Switching "on" and "off" the Adhesion in Stimuli-responsive Elastomers. *Soft Matter* **2018**, *14*, 2547−2559.

(10) Wang, W.; Xiang, C.; Zhu, Q.; Zhong, W.; Li, M.; Yan, K.; Wang, D. Multistimulus Responsive Actuator with GO and Carbon Nanotube/PDMS Bilayer Structure for Flexible and Smart Devices. *ACS Appl. Mater. Interfaces* **2018**, *10*, 27215−27223.

(11) Zhan, Z.; Lin, R.; Tran, V.-T.; An, J.; Wei, Y.; Du, H.; Tran, T.; Lu, W. Paper/Carbon Nanotube-Based Wearable Pressure Sensor for Physiological Signal Acquisition and Soft Robotic Skin. *ACS Appl. Mater. Interfaces* **2017**, *9*, 37921−37928.

(12) Liu, Y.; Du, H.; Liu, L.; Leng, J. Shape Memory Polymers and Their Composites in Aerospace Applications: a Review. *Smart Mater. Struct.* **2014**, *23*, No. 023001.

(13) Gladman, A. S.; Matsumoto, E. A.; Nuzzo, R. G.; Mahadevan, L.; Lewis, J. A. Biomimetic 4D printing. *Nat. Mater.* **2016**, *15*, 413−418.

(14) Huang, L.; Jiang, R.; Wu, J.; Song, J.; Bai, H.; Li, B.; Zhao, Q.; Xie, T. Ultrafast Digital Printing toward 4D Shape Changing Materials. *Adv. Mater.* **2017**, *29*, No. 1605390.

(15) Zhao, Q.; Qi, H. J.; Xie, T. Recent Progress in Shape Memory Polymer: New Behavior, Enabling Materials, and Mechanistic Understanding. *Prog. Polym. Sci.* **2015**, *49*−*50*, 79−120.

(16) Meng, H.; Li, G. Reversible Switching Transitions of Stimuli-responsive Shape Changing Polymers. *J. Mater. Chem. A* **2013**, *1*, 7838−7865.

(17) Liu, Y.; Shaw, B.; Dickey, M. D.; Genzer, J. Sequential Self-folding of Polymer Sheets. *Sci. Adv.* **2017**, *3*, No. e1602417.

(18) Chen, Z.; Guo, Q.; Majidi, C.; Chen, W.; Srolovitz, D. J.; Haataja, M. P. Nonlinear Geometric Effects in Mechanical Bistable Morphing Structures. *Phys. Rev. Lett.* **2012**, *109*, No. 114302.

(19) Yang, Y.; Terentjev, E. M.; Wei, Y.; Ji, Y. Solvent-assisted Programming of Flat Polymer Sheets into Reconfigurable and Self-healing 3D Structures. *Nat. Commun.* **2018**, *9*, No. 1906.

(20) Yan, Z.; Zhang, F.; Wang, J.; Liu, F.; Guo, X.; Nan, K.; Lin, Q.; Gao, M.; Xiao, D.; Shi, Y.; et al. Controlled Mmechanical Buckling for Origami-inspired Construction of 3D Microstructures in Advanced Materials. *Adv. Funct. Mater.* **2016**, *26*, 2629−2639.

(21) Yuan, C.; Roach, D. J.; Dunn, C. K.; Mu, Q.; Kuang, X.; Yakacki, C. M.; Wang, T.; Yu, K.; Qi, H. J. 3D Printed Reversible Shape Changing Soft Actuators Assisted by Liquid Crystal Elastomers. *Soft Matter* **2017**, *13*, 5558−5568.

(22) Peng, X.; Li, Y.; Zhang, Q.; Shang, C.; Bai, Q. W.; Wang, H. Tough Hydrogels with Programmable and Complex Shape Deformations by Ion Dip-Dyeing and Transfer Printing. *Adv. Funct. Mater.* **2016**, *26*, 4491−4500.

(23) Mailen, R. W.; Liu, Y.; Dickey, M. D.; Zikry, M.; Genzer, J. Modelling of Shape Memory Polymer Sheets that Self-fold in Response to Localized Heating. *Soft Matter* **2015**, *11*, 7827−7834.

(24) Zhang, Y.; Yan, Z.; Nan, K.; Xiao, D.; Liu, Y.; Luan, H.; Fu, H.; Wang, X.; Yang, Q.; Wang, J.; et al. A Mechanically Driven form of Kirigami as a Route to 3D Mesostructures in Micro/nanomembranes. *Proc. Natl. Acad. Sci. U.S.A.* **2015**, *112*, 11757−11764.

(25) Ko, H.; Javey, A. Smart Actuators and Adhesives for Reconfigurable Matter. *Acc. Chem. Res.* **2017**, *50*, 691−702.

(26) Xie, T. Tunable Polymer Multi-shape Memory Effect. *Nature* **2010**, *464*, 267−270.

(27) Sperling, L. H. *Introduction to Physical Polymer Science*; John Wiley & Sons, 2005.

(28) Yu, X.; Zhang, L.; Hu, N.; Grover, H.; Huang, S.; Wang, D.; Chen, Z. Shape Formation of Helical Ribbons Induced by Material Anisotropy. *Appl. Phys. Lett.* **2017**, *110*, No. 091901.

(29) Liu, J.; Huang, J.; Su, T.; Bertoldi, K.; Clarke, D. R. Structural Transition from Helices to Hemihelices. *PLoS One* **2014**, *9*, No. e93183.